Int. J. Solids Structures, 1977, Vol 13, pp 395–407. Pergamon Press Printed in Great Britain

APPLICATION OF A DISCRETE POLYCRYSTAL MODEL TO THE ANALYSIS OF CYCLIC STRAINING IN COPPER

K. S HAVNER
Department of Civil Engineering, North Carolina State University, Raleigh, NC 27607, U.S.A.

and

C. SINGH
Department of Civil Engineering, Bucknell University, Lewisburg, PA 17837, U.S A.

(*Received* 29 *July* 1976; *revised* 3 *September* 1976)

Abstract—A discrete polycrystal model, designed to simulate a metal aggregate macro-element, is applied to the study of cyclic straining in copper. The numerical method of solution (an adaptation of the "finite element method") incorporates a convergent discrete Green's function within the constrained minimum principle which governs the (crystallographic) plastic shear increments at each load step. Isothermal elastic moduli of copper crystals and Taylor's hardening rule with constant hardening modulus are used in the calculations. Numerical results are obtained for macroscopic elastic properties, cyclic stress-strain curves (which indicate the contribution of aggregate heterogeneity to macroscopic hardening), macroscopic plastic work, and residual (latent) strain energy through four loading cycles between fixed macrostrain limits. Other estimates for elastic properties also are included, and all results are compared, both qualitatively and quantitatively, with published experiments. The predictions of the model are in general satisfactory.

1 INTRODUCTION

This work deals with the application of a discrete crystalline aggregate model proposed by Havner[1] to the study of cyclic straining in copper. The model, in brief, consists of a "unit" polycrystalline cube (say 1 mm^3) simulating an aggregate volume cut *through the thickness* of a flat sheet or thin-walled tube specimen. Uniform normal displacements (corresponding to macroscopically homogeneous strain) are imposed on two pairs of opposite faces while the third pair are free. The variously oriented crystals are taken to be symmetrically disposed with respect to bisecting planes of the cube so that only one quadrant is analyzed. Within that quadrant the elastically anisotropic grains (here numbering approximately 100) are so distributed with regard to lattice orientation as to closely approximate macroscopic isotropy. For a given biaxial macrostrain history, the model predicts the accompanying biaxial macroscopic stresses, distributions of active slip systems, macroscopic plastic strains, total plastic work, and residual (latent) strain energy.

The calculations at each incremental step are separated into the analysis of a purely elastic boundary value problem and the analysis of a self-straining problem in the unknown crystallographic shear rates. The latter calculations are made feasible through a numerical "Green's function" approach which is presented in detail in the Appendix. The elastic part of the problem is determined through the evaluation of numerical macrostrain influence functions as shown in Section 2. The uniqueness and minimum principles which govern the incremental plastic shears in the self-straining problem are reviewed in Section 3, followed in Section 4 by equations for macroscropic stresses, work and energy. These latter quantities are evaluated for cyclic straining of the aggregate model in Section 5.

The principal numerical results may be briefly summarized as follows. The model's predictions for macroscopic elastic properties, aggregate hardening from single crystal hardening, and percentage of plastic work stored as latent strain energy are in good agreement with experiment. The predicted cyclic stress-strain curves (through four strain cycles) exhibit a significant Bauschinger effect and suggest a trend toward a stable hysteresis loop, but these features of the model's behavior are less pronounced than would be the corresponding characteristics observed experimentally in copper.

The purely elastic response of the model also is compared with the classical Reuss and Voigt bounds and the "self-consistent" estimates for aggregate properties. In the cyclic plastic

range, however, we are not aware of other numerical studies fully incorporating crystal anisotropy, slip system hardening, aggregate heterogeneity, and latent energy with which comparisons can be made.

2. ELASTIC ANALYSIS OF THE AGGREGATE MODEL

2.1 *General*

The present polycrystal computations, like those in Havner and Varadarajan[2] and Havner *et al.*[3], are based upon the use of piecewise linear interpolating polynomials for local displacement fields. Moreover, we adopt the simplest admissible finite element representation of the aggregate model by choosing each tetrahedral element to simulate an entire grain. Clearly, this approximation (uniform strain within each crystal) cannot be expected to yield particularly accurate results for local fields. However, because the macroscopic quantities we seek to determine (e. g. stress, plastic work, latent energy) are *global averages*, we believe the corresponding calculations are reasonably representative of the theoretical behavior of the aggregate. One basis for this conclusion is the satisfactory elastic response of the numerical model, as shown here and in the next sub-section.

Because the aggregate model corresponds to a macroscopic state of (biaxial) plane stress $\bar{\sigma}_{11}, \bar{\sigma}_{22}$, the elastic part of the problem is solved once and for all by determining the local (elastic) strain influence functions $\boldsymbol{\psi}_1(x)$, $\boldsymbol{\psi}_2(x)$ caused by separately imposed macroscopic strains $\bar{\epsilon}_{11} = 1$, $\bar{\epsilon}_{22} = 1$. (The A_3 faces of the unit cube are free and the A_1, A_2 faces are *tangentially* unconstrained.) Then, for arbitrary increments $\delta\bar{\epsilon}_{11}$, $\delta\bar{\epsilon}_{22}$,

$$\delta\boldsymbol{\epsilon}_e(x) = \delta\bar{\epsilon}_{11}\boldsymbol{\psi}_1(x) + \delta\bar{\epsilon}_{22}\boldsymbol{\psi}_2(x). \tag{2.1}$$

(The subscript e denotes the elastic part of the incremental boundary value problem and *not* the final elastic strain increment.) Further, from strain energy considerations, the symmetric, macroscopic *plane stress* moduli $\mathscr{L}_{\alpha\beta}$ can be calculated as [1, eqn (4.7)]

$$\mathscr{L}_{\alpha\beta} = \int (\psi_{ij})_\alpha \mathscr{L}_{ijkl} (\psi_{kl})_\beta \, \mathrm{d}V, \quad \alpha, \beta = 1, 2, \tag{2.2}$$

where the local tensor of crystal elastic moduli is positive-definite with symmetries $\mathscr{L}_{ijkl} = \mathscr{L}_{jikl} = \mathscr{L}_{klij}$. For a sufficiently random distribution of crystal orientations, such that the macroscopic response is nearly isotropic and $\mathscr{L}_{11} \approx \mathscr{L}_{22}$, the modulus of elasticity and Poisson's ratio in the $x_1 - x_2$ "plane" may be calculated from

$$\left.\begin{aligned} E &= \frac{1}{2}(\mathscr{L}_{11}\mathscr{L}_{22} - \mathscr{L}_{12}\mathscr{L}_{21})(1/\mathscr{L}_{11} + 1/\mathscr{L}_{22}), \\ \nu &= \frac{1}{2}\mathscr{L}_{12}(1/\mathscr{L}_{11} + 1/\mathscr{L}_{22}). \end{aligned}\right\} \tag{2.3}$$

The exact influence functions $\boldsymbol{\psi}_1(x)$, $\boldsymbol{\psi}_2(x)$ are determined (in principle) by minimization of

$$2I_1(\mathbf{v}) = \int \partial\mathbf{v} \cdot \mathscr{L} \cdot \partial\mathbf{v} \, \mathrm{d}V \tag{2.4}$$

on the class of continuous displacements satisfying $v_1 = \pm 1/2$ on faces A_1, $v_2 = 0$ on faces A_2, and the opposite. ($\partial\mathbf{v}$ denotes the symmetric part of the spatial gradient of displacement field $\mathbf{v}(x)$, and $\mathscr{L}$ is the local tensor of crystal elastic moduli.) Thus, because the finite-element polynomials belong to the admissible class,

$$\mathscr{L}^h_{\alpha\alpha} = \int \boldsymbol{\psi}_\alpha{}^h \cdot \mathscr{L} \cdot \boldsymbol{\psi}_\alpha{}^h \, \mathrm{d}V \geq \mathscr{L}_{\alpha\alpha} = \int \boldsymbol{\psi}_\alpha \cdot \mathscr{L} \cdot \boldsymbol{\psi}_\alpha \, \mathrm{d}V, \quad \alpha = 1, 2, \tag{2.5}$$

(no sum on α) where $\boldsymbol{\psi}_\alpha{}^h$ is the finite-element solution for the influence function $\boldsymbol{\psi}_\alpha$. Modulus $\mathscr{L}^h_{12}$, however, is not necessarily an upper bound to $\mathscr{L}_{12} = \mathscr{L}_{21}$, and it is likely from (2.3), (2.5) (but we

cannot prove) that E^h is an upper bound to E. (As shown in the following, E^h is close to and greater than published *experimental* values.)

2.2 *Quantitative model and numerical results*

A quadrant of the unit polycrystalline cube adopted for our calculations is shown in Fig. 1. Each of the 16-sub-cubes of the quadrant is divided into 6 tetrahedral crystallites, each of a different orientation. Thus there are a total of 384 crystallites within the unit cube and 4608 crystallographic slip systems, 1152 within the quadrant. (A consideration of computer time and storage requirements for the large numbers of potentially active slip systems in the subsequent *plastic* analysis has determined our choice of this relatively coarse aggregate model.)

The specific Euler angles selected for the 96 crystallites within the quadrant (corresponding to the nodal numbering scheme indicated in Fig. 1) are given in Singh [4, Table 1]. The distribution of orientations is not truly random but was selected (after several trials) with the single objective of achieving satisfactory overall isotropic response of the model. For example, pairs of crystallites similarly placed on the two sides of the diagonal plane bisecting the quadrant are symmetrically oriented with respect to the diagonal. Certain changes are abrupt, but for the most part orientations vary by only a few degrees from grain to grain. The ranges of the Euler angles ϕ, θ, ψ are respectively $\pm 12°$ through $\pm 55°$, $\pm 7°$ through $\pm 48°$, and $\pm 16°$ through $\pm 63°$ (refer to [2, Fig. A1] for definitions).

The values used for the elastic constants of copper crystals are (in Voigt notation): $c_{11} = 1.641 \times 10^{11}$, $c_{12} = 1.174 \times 10^{11}$, $c_{44} = 0.751 \times 10^{11}$ N/m^2. These are isothermal moduli evaluated according to eqns (6) in Barsch[5] from the adiabatic constants and bulk moduli of copper given in Barsch and Chang[6]. The isothermal bulk modulus is $K = (c_{11} + 2c_{12})/3 = 1.330 \times 10^{11}$ N/m^2.

The results of the calculations for discrete influence functions ψ_1, ψ_2 (henceforth suppressing the suffix h) give for the macroscopic moduli (from 2.2): $\mathscr{L}_{11} = 1.434 \times 10^{11}$, $\mathscr{L}_{12} = \mathscr{L}_{21} = 0.511 \times 10^{11}$, $\mathscr{L}_{22} = 1.448 \times 10^{11}$ N/m^2. The values $\mathscr{L}_{11}$ and $\mathscr{L}_{22}$ differ by less than 1%, indicating a distribution of orientations sufficient to approximately represent statistical isotropy. Upon substitution into (2.3) we find $E = 1.260 \times 10^{11}$ N/m^2 and $\nu = 0.355$, from which $G = E/2(1+\nu) = 0.465 \times 10^{11}$ N/m^2. Alternatively, since $\mathscr{L}_{11} \approx \mathscr{L}_{22}$, the shear modulus in the $x_1 - x_2$ plane can be calculated from

$$G = (\mathscr{L}_{11}\mathscr{L}_{22} - \mathscr{L}_{12}\mathscr{L}_{21})/(\mathscr{L}_{11} + \mathscr{L}_{22} + 2\mathscr{L}_{12}), \tag{2.6}$$

which also gives $G = 0.465 \times 10^{11}$ N/m^2. (Equations (2.3) and (2.6) do not satisfy exactly the isotropic relation $G = E/2(1+\nu)$ unless $\mathscr{L}_{11} = \mathscr{L}_{22}$. For the present values, however, the two definitions of (averaged) modulus G differ only by one in the fourth significant figure.)

The macroscopic bulk modulus is precisely the same as the single crystal value, $K =$

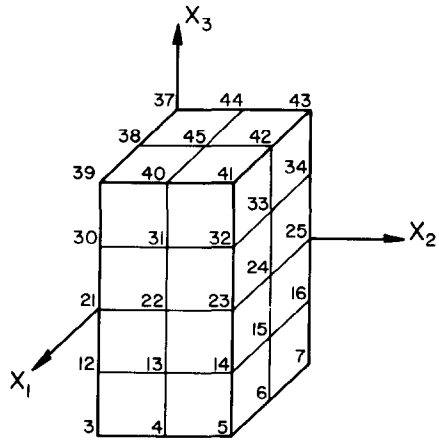

Fig. 1. Quadrant of unit polycrystalline cube.

1.330×10^{11} N/m^2, because the response of cubic crystals to pressure is isotropic. Correspondingly, another set of (averaged) values for E and ν may be calculated using G from (2.6) and the exact K so as to satisfy the isotropic relations

$$E = 9KG/(3K+G), \quad \nu = \frac{1}{2}(3K-2G)/(3K+G). \tag{2.7}$$

These give $E = 1.249 \times 10^{11}$ N/m^2 and $\nu = 0.343$, which differ from the previous values by approximately one and 3% respectively.

There is no unanimity in the literature regarding *experimental* values of the macroscopic properties of polycrystalline copper. A set of constants from averaged data naturally must satisfy (2.7) to be representative of statistically isotropic material. Moreover, for comparison with our results we consider only published sets of constants whose respective bulk moduli equal the (rounded) value $K = 1.33 \times 10^{11}$ N/m^2 calculated from the single crystal moduli adopted here. Two sets of experimental values which meet these conditions are: $K = 1.33 \times 10^{11}$, $G = 0.436 \times 10^{11}$, $E = 1.18 \times 10^{11}$ N/m^2 and $\nu = 0.352$ from [7]; and $K = 1.33 \times 10^{11}$, $G = 0.455 \times 10^{11}$, $E = 1.23 \times 10^{11}$ N/m^2 and $\nu = 0.346$ from [8]. Our computed values for E and G differ from the first set of experimental constants by 6 to 7% and from the second set by 2%. The two computed values of Poisson's ratio differ from the experimental values by from 1 to 3%.

It is of interest to compare the present results with the Reuss and Voigt bounds (cf. Hill[7]) and the "self-consistent" model (see Hutchinson[9]), all of which are analytical estimates of polycrystalline elastic moduli. Using the same elastic constants of copper crystals as here, all three (of course) give the exact bulk modulus $K = 1.330 \times 10^{11}$ N/m^2, in agreement with experiment. For shear modulus G, the Voigt and Reuss bounds are[7]

$$G_V = \frac{1}{5}(c_{11} - c_{12} + 3c_{44}), \quad G_R = \frac{5}{4(s_{11} - s_{12}) + 3s_{44}}, \tag{2.8}$$

where $s_{11} - s_{12} = 1/(c_{11} - c_{12})$ and $s_{44} = 1/c_{44}$ are the crystal compliances. Thus, $G_V = 0.544 \times 10^{11}$ N/m^2 and $G_R = 0.398 \times 10^{11}$ N/m^2. Correspondingly, the bounds on E and ν are (from (2.7)): $E_R = 1.086 \times 10^{11} < E < 1.436 \times 10^{11} = E_V$; $\nu_V = 0.320 < \nu < 0.364 = \nu_R$.

The shear modulus of the "self-consistent" model is determined from the cubic equation[9]

$$8G^3 + (5c_{11} + 4c_{12})G^2 - (7c_{11} - 4c_{12})c_{44}G - (c_{11} - c_{12})(c_{11} + 2c_{12})c_{44} = 0, \tag{2.9}$$

which gives $G = 0.479 \times 10^{11}$ N/m^2, whence $E = 1.283 \times 10^{11}$ N/m^2 and $\nu = 0.339$ from (2.7). The "self-consistent" results for E, G and ν respectively differ from the first set of experimental values by 8.5, 10 and 4% and from the second set by 4, 5 and 2%

The various values for elastic constants are summarized in Table 1. Overall, our calculated isotropic values agree with the widely accepted "self-consistent" predictions to within 3%.

Table 1. Comparison of various estimates for isotropic elastic constants of copper with experimental values

	K	G	E	ν	
Experiment	1.33	0.436	1.18	0.352	Hill [7]
	1.33	0.455	1.23	0.346	Hearmon [8]
Present Model	1.330	0.465	1.249	0.343	(2.6) and (2.7)
	1.330	0.465	1.260	0.355	(2.3)*
Reuss	1.330	0.398	1.086	0.364	(2.8_1) and (2.7)
Self-Consistent	1.330	0.479	1.283	0.339	(2.9) and (2.7)
Voigt	1.330	0.544	1.436	0.320	(2.8_2) and (2.7)

Units = 10^{11}N/m^2

*These values do not satisfy identically the isotropic relations (2.7).

[Hashin and Shtrikman [10] present a set of relations (their eqns (3.30)–(3.34)) stated to be upper and lower bounds to the isotropic shear modulus G which are closer than the Voigt and Reuss bounds. For the values of single crystal moduli adopted here we obtain $0.457\times10^{11}<G<0.492\times10^{11}$ N/m^2 using their equations, a relatively narrow range which includes both the "self-consistent" value and our approximate result for G (but not the reported values in [7, 8]). Kröner, Datta and Kessel [11] have cited Hashin and Shtrikman's equations and accepted their correctness, presenting them in a different but algebraically equivalent form. However, the lower bound eqn (3.30) in [10] is not consistent with eqn (3.25) therein from which it reportedly is derived. Thus, we are not certain whether Hashin and Shrikman's relations are analytically rigorous bounds.]

3. ANALYSIS OF CRYSTALLOGRAPHIC PLASTIC SHEARING

In the application of our polycrystal model to the study of cyclic straining in copper, we have adopted the classical and widely used Taylor hardening rule (Taylor [12, 13]). Further, we have assumed a constant slip system hardening modulus H (see Section 5). Thus, the current value of critical strength in each of the slip systems at a crystal material point is

$$\tau_{cr}=\tau_0+H\sum\int\delta\gamma_k. \tag{3.1}$$

Here, opposite senses of slip in the same crystallographic system are denoted by distinct k's so that $\delta\gamma_k$ is always nonnegative, and the summation is made over all systems. (τ_0 denotes the initial shear strength of the unstrained crystal.)

In a *critical* slip system the local resolved shear stress $\mathbf{N}^k\cdot\boldsymbol{\sigma}=\tau_{cr}$, where $\mathbf{N}^k$ is the symmetric part of the dyadic product $(\mathbf{b}\otimes\mathbf{n})^k$, $\mathbf{n}^k$ and $\mathbf{b}^k$ denoting unit vectors in the normal and glide directions respectively of the kth system. The critical slip system constitutive relations thus may be written

$$\mathbf{N}^k\cdot\dot{\boldsymbol{\sigma}}\le H\sum\dot\gamma_j,\quad\dot\gamma\ge0, \tag{3.2}$$

$$\dot\gamma_k\mathbf{N}^k\cdot\dot{\boldsymbol{\sigma}}=\dot\gamma_kH\sum\dot\gamma_j\quad\text{(for each }k\text{)}, \tag{3.3}$$

in which the dot above denotes material differentiation with respect to a time-like variable. (Alternatively, the dot may be taken as representing an increment in the quantity.) The stress rate is obtained by superposition of the elastic solution of Section 2 with the solution of the "self-straining" problem from the Appendix:

$$\dot{\boldsymbol{\sigma}}(x)=\mathscr{L}\cdot\dot{\boldsymbol{\epsilon}}_e(x)-\int\mathbf{Z}(x,x')\cdot\dot{\boldsymbol{\epsilon}}^I(x')\,dV', \tag{3.4}$$

where

$$\dot{\boldsymbol{\epsilon}}_e=\dot{\bar\epsilon}_{11}\boldsymbol{\psi}_1+\dot{\bar\epsilon}_{22}\boldsymbol{\psi}_2,\quad\dot{\boldsymbol{\epsilon}}^I=\sum\mathbf{N}^j\dot\gamma_j, \tag{3.5}$$

and the discrete influence function $\mathbf{Z}(x,x')$ is given by (A12). (Recall that $\dot{\bar\epsilon}_{11}$, $\dot{\bar\epsilon}_{22}$ are *prescribed* by imposing appropriate normal displacement rates on faces A_1, A_2 of the unit cube.) Upon substitution of (3.4) into (3.2) and (3.3) (integrating the latter over V after summing on the critical systems within each crystal),

$$\mathbf{N}^k\cdot\dot{\boldsymbol{\sigma}}_e(x)\le H\sum\dot\gamma_j(x)+\int\mathbf{N}^k(x)\cdot\mathbf{Z}(x,x')\cdot\sum\mathbf{N}^j\dot\gamma_j(x')\,dV', \tag{3.6}$$

$$\int\sum\gamma_k\mathbf{N}^k\cdot\dot{\boldsymbol{\sigma}}_e\,dV=\int H\Big(\sum\dot\gamma_k\Big)^2dV+\int\int\sum\sum\dot\gamma_k(x)p^{kj}(x,x')\dot\gamma_j(x')\,dV'\,dV, \tag{3.7}$$

where $\dot{\boldsymbol{\sigma}}_e=\mathscr{L}\cdot\dot{\boldsymbol{\epsilon}}_e$ and

$$p^{kj}(x,x')=\mathbf{N}^k(x)\cdot\mathbf{Z}(x,x')\cdot\mathbf{N}^j(x'), \tag{3.8}$$

with $p^{kj}(x, x') = p^{jk}(x', x)$ from (A6). (For the finite element approximation adopted here, x and x' may be understood to denote crystallites rather than points since discrete stresses, total strains and plastic shears are spatially uniform within each grain.)

Equations (3.6), (3.7) and the requirement $\dot{\gamma}_k(x) \geq 0$ for all k constitute a "linear complementarity problem" in the unknown plastic shear rates which is equivalent to the following constrained minimization problem (see Havner[1] or Maier[14]). Minimize

$$2I(\dot{\boldsymbol{\lambda}}) = \int H\Big(\sum \dot{\lambda}_k\Big)^2 \,\mathrm{d}V + \int\int \sum\sum \dot{\lambda}_k(x) p^{kj}(x, x') \dot{\lambda}_j(x') \,\mathrm{d}V' \,\mathrm{d}V - 2\int \sum \dot{\lambda}_k \mathbf{N}^k \cdot \dot{\boldsymbol{\sigma}}_e \,\mathrm{d}V \tag{3.9}$$

on the class of *nonnegative* plastic multiplier rates $\dot{\lambda}_k$ in critical systems. The corresponding uniqueness condition is

$$\int H\Big(\sum \dot{\lambda}_k\Big)^2 \,\mathrm{d}V + \int\int \sum\sum \dot{\lambda}_k(x) p^{kj}(x, x') \dot{\lambda}_j(x') \,\mathrm{d}V' \,\mathrm{d}V > 0 \tag{3.10}$$

for *all* plastic multipliers $\dot{\lambda}_k$ in critical systems. From (A1, A4, 3.5$_2$) and the virtual work equation of the self-straining problem, $\int \dot{\boldsymbol{\sigma}}_s \cdot \partial \mathbf{w} \,\mathrm{d}V = 0$, we find

$$\int\int \sum\sum \dot{\gamma}_k(x) p^{kj}(x, x') \dot{\gamma}_j(x') \,\mathrm{d}V' \,\mathrm{d}V = \int \dot{\boldsymbol{\sigma}}_s \cdot \mathscr{L}^{-1} \cdot \dot{\boldsymbol{\sigma}}_s \,\mathrm{d}V > 0 \tag{3.11}$$

without regard to the signs of the $\dot{\gamma}$'s, so long as the $\mathbf{N}^k$ are linearly independent† (i.e. no more than five critical slip systems within each crystal). Thus, the solution is unique for $H \geq 0$ and the unknown plastic shear rates $\dot{\gamma}_k$ equal the nonnegative $\dot{\lambda}$'s which minimize the functional $I(\dot{\boldsymbol{\lambda}})$. (For a more comprehensive discussion of the matter of uniqueness, refer to Havner[15].)

4. MACROSCOPIC STRESS, WORK AND ENERGY

Once the incremental plastic shears (or shear rates) are calculated from (3.9) for prescribed macroscopic strain increments $\delta\bar{\epsilon}_{11}$, $\delta\bar{\epsilon}_{22}$, the local stress increments are determined from (3.4), and the macroscopic stress increments are calculated as

$$\delta\bar{\sigma}_{11} = \int \delta\sigma_{11}(x) \,\mathrm{d}V, \quad \delta\bar{\sigma}_{22} = \int \delta\sigma_{22}(x) \,\mathrm{d}V. \tag{4.1}$$

As shown in Havner[1] (also refer to Hill[16]), these equations are consistent with the operational definition of macroscopic stress $\bar{\sigma}_{ij}$ as the average of traction $t_j = n_i\sigma_{ij}$ acting on face A_i of the unit cube. Thus, all other volume averages of local stress components should be zero corresponding to the boundary conditions defined in Section 2. However, because of the numerical approximations introduced through the chosen finite element discretization, small nonzero values of these other integrals actually can be calculated, but these are disregarded here.

The operational definitions of macroscopic plastic strain increments (corresponding to the macroscopic *plane stress* moduli $\mathscr{L}_{\alpha\beta}$) are

$$\left.\begin{aligned} \delta\bar{\epsilon}^p_{11} &= \delta\bar{\epsilon}_{11} - \mathscr{C}_{11}\delta\bar{\sigma}_{11} - \mathscr{C}_{12}\delta\bar{\sigma}_{22}, \\ \delta\bar{\epsilon}^p_{22} &= \delta\bar{\epsilon}_{22} - \mathscr{C}_{21}\delta\bar{\sigma}_{11} - \mathscr{C}_{22}\delta\bar{\sigma}_{22}, \end{aligned}\right\} \tag{4.2}$$

where

$$\left.\begin{aligned} \mathscr{C}_{11} &= \mathscr{L}_{22}/(\mathscr{L}_{11}\mathscr{L}_{22} - \mathscr{L}_{12}\mathscr{L}_{21}), \\ \mathscr{C}_{12} &= -\mathscr{L}_{12}/(\mathscr{L}_{11}\mathscr{L}_{22} - \mathscr{L}_{12}\mathscr{L}_{21}) = \mathscr{C}_{21}, \\ \mathscr{C}_{22} &= \mathscr{L}_{11}/(\mathscr{L}_{11}\mathscr{L}_{22} - \mathscr{L}_{12}\mathscr{L}_{21}). \end{aligned}\right\} \tag{4.3}$$

†If the $\mathbf{N}^k$ were not linearly independent, then from (3.5$_2$) there conceivably could be nonnegative $\dot{\gamma}$'s producing identically zero $\dot{\boldsymbol{\epsilon}}^t$, whence zero $\dot{\boldsymbol{\sigma}}_s$ from (A1).

Thus, macroscopic (mechanically irrecoverable) *apparent* plastic work is determined as

$$W_P = \int (\bar{\sigma}_{11}\delta\bar{\epsilon}^P_{11} + \bar{\sigma}_{22}\delta\bar{\epsilon}^P_{22}), \tag{4.4}$$

or, alternatively, as $W - W_E$ where

$$W = \int (\bar{\sigma}_{11}\delta\bar{\epsilon}_{11} + \bar{\sigma}_{22}\delta\bar{\epsilon}_{22}) \tag{4.5}$$

and

$$W_E = \frac{1}{2}\mathscr{C}_{11}\bar{\sigma}^2_{11} + \mathscr{C}_{12}\bar{\sigma}_{11}\bar{\sigma}_{22} + \frac{1}{2}\mathscr{C}_{22}\bar{\sigma}^2_{22} \tag{4.6}$$

are respectively total work and apparent elastic work over the unit cube. The (internal) elastic strain energy stored within the cube is

$$U = \frac{1}{2}\int \boldsymbol{\sigma} \cdot \mathscr{L}^{-1} \cdot \boldsymbol{\sigma}\, \mathrm{d}V, \tag{4.7}$$

which exceeds W_E by an amount U_R called the residual or latent strain energy. Here, as in Havner *et al.*[3], we choose to directly calculate the internal plastic work

$$Q = \int \left(\int \boldsymbol{\sigma} \cdot \sum \mathbf{N}^k \delta\gamma_k \right) \mathrm{d}V = \tau_0 \int \left(\sum \gamma_k \right) \mathrm{d}V + \frac{1}{2} H \int \left(\sum \gamma_k \right)^2 \mathrm{d}V \tag{4.8}$$

and obtain U, U_R, and W_e from

$$U = W - Q, \quad U_R = W_P - Q, \quad W_E = W - W_P. \tag{4.9}$$

Within the limitations of the present continuum theory of crystallographic shearing, the internal plastic work Q is identified with mechanical energy dissipated as hear under adiabatic conditions. A portion of such work, however, is generally understood to be stored as a *sub*microscale strain energy associated with newly created dislocations, as first suggested by Taylor[17]. Therefore, the total latent energy is a combination of this submicroscale energy and the residual energy U_R, with the present theory and model capable of predicting (and calculating) only the latter. (U_R is of course the energy of *gross* lattice straining in the polycrystalline aggregate at zero macrostress—that is, the strain energy of the corresponding self-equilibrated microstress field.)

5. QUANTITATIVE RESULTS IN CYCLIC STRAINING

5.1 *Cyclic stress-strain curves*

A value of 1.177×10^8 N/m^2 (12 kgf/mm^2) was chosen for the slip system hardening modulus H. This value is a representative average taken from single crystal resolved shear stress-strain curves in Kemsley and Paterson[18]. It also is consistent with average values in the low to moderate strain range from single crystal curves in Williams[19]. The value of τ_0 is immaterial since we have chosen to display final results as stress/$2\tau_0$, strain/$(2\tau_0/E)$, and work per unit volume/$(4\tau_0^2/E)$. These dimensionless quantities depend only upon the parameter H/E (here approximately equal to 10^{-3}), as discussed in Havner and Varadarajan[2].

In each calculation for incremental plastic shears through minimization of (3.9), the method of Hildreth and D'Esopo (see Künzi and Krelle[20]) was used.† For a prescribed ratio $\delta\bar{\epsilon}_{11} : \delta\bar{\epsilon}_{22}$,

†A gradient method due to De Donato and Franchi[21] also was tried but was not adopted based upon comparative studies by Singh[4].

the incremental solution was first obtained for arbitrary amounts ($\delta\bar{\epsilon}_{11} = 1$, say). All increments were then scaled down to the level at which $\mathbf{N}^k \cdot (\boldsymbol{\sigma} + \delta\boldsymbol{\sigma})$ just reached the critical strength $\tau_{cr} + \delta\tau_{cr}$ in the next potentially active system. (As a practical matter, all systems having resolved shear stresses at least 99.9% of their respective critical strengths were included as critical systems within each increment. For further discussion of the computational procedures, refer to Singh[4].)

Calculations were carried-out through four complete cycles of uniaxial stressing $\bar{\sigma}_{11}$ between fixed strain limits $\bar{\epsilon}_{11}/(2\tau_0/E) = 0$ and 14.2, using nearly 1400 incremental steps. The resulting computer-plotted, cyclic stress-strain curves are displayed in Figure 2. The maximum "strain" value 14.2 is approximately 15 times the strain at point A corresponding to the initiation of plastic slip within the model. To maintain uniaxial stress corresponding to macrostrain inputs, it was necessary to frequently adjust the ratio $\delta\bar{\epsilon}_{11} : \delta\bar{\epsilon}_{22}$ so as to hold $\bar{\sigma}_{22}$ close to zero. The actual small oscillations of this stress about zero are shown as superimposed wavy lines lying along the strain axis.

Points marking the onset of plastic deformation within each half-cycle (i.e. the end of a purely elastic interval) are labeled alphabetically, in sequence, in Fig. 2. *Pronounced* plastic straining does not begin, however, until about one-fourth of the total number of possible critical systems are active. (We suppose five to be the maximum number of simultaneously active slip systems per grain, giving 480 possible critical systems within a quadrant of the model.) The number of active systems increases rapidly and at peak stress points approximately three-fourths of the possible systems are active. For example, there are 361 active slip systems at the end of the first loading half-cycle (refer to Table 1 in Singh[4]), and 61% of the crystals have 4 or 5 active systems (96% have at least three active systems).

Since our calculations are based upon Taylor hardening, which does not account for a Bauschinger effect within individual crystals, the *macroscopic* Bauschinger effect observed in Fig. 2 is due entirely to the non-uniformity of local stresses within the heterogeneous aggregate. That such an effect is to be expected in the polycrystal model even for Taylor hardening was shown analytically in Havner[1]. It seems evident that a stronger macroscopic Bauschinger effect would be obtained, as is observed experimentally, were a crystal hardening rule adopted incorporating this effect within each grain. (To the writers' knowledge, the only such rule that has been calculated is the translational hardening of Budiansky and Wu[22].)

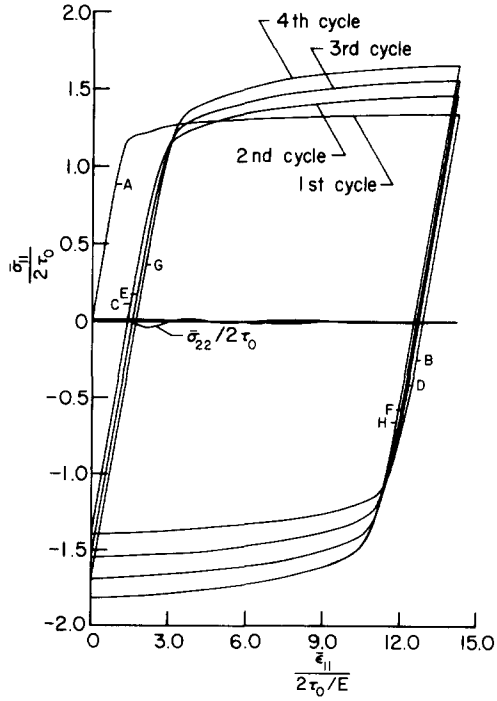

Fig. 2. Dimensionless cyclic stress-strain curves for polycrystal model of copper.

Another generally observed phenomenon in cyclic straining of polycrystalline copper is the evolution of a repeating (constant) hysteresis loop after a large number of tension and compression cycles (of the order several hundreds). The aggregate "hardening" per cycle increases at a decreasing rate and eventually reaches a saturation state. We cannot expect to observe this phenomenon of a constant hysteresis loop in the small number of cycles calculated here. However, our model exhibits a trend in that direction in one respect. Upon comparing the peak stresses at the ends of successive loading and reverse loading half-cycles (Fig. 2), the following percent increases (per cycle) are found: in loading, 8.94, 6.63, 6.35; in reverse loading, 11.2, 8.85, 7.54. These decreasing percentages suggest that, even with the adoption of Taylor hardening and a constant modulus H, the model's response may tend toward real polycrystalline behavior after a large number of cycles. On the other hand, the (average) tangent moduli near the ends of the half-cycles are slightly increasing, suggesting the converse. To resolve the matter, of course, would require the evaluation of many more cycles. It may be that the model's response cannot show a strong trend toward a stable hysteresis loop unless one adopts a modulus H which is a decreasing function of accumulative plastic shears (rather than a constant as here).

From Fig. 2, the mean of the (average) tangent moduli in the intervals of significant plastic straining is approximately $E_T/E = 1.2 \times 10^{-2}$. Hence, *the aggregate heterogeneity produces an order-of-magnitude increase in hardening above the single crystal hardening* (i.e. $E_T/E \approx 12H/E$). This is in satisfactory agreement with the average values, in the low to moderate strain range, from polycrystalline copper stress-strain curves in Williams[23] and Wolfenden[24] and single crystal curves in Williams[19]. Thus, the aggregate model appears to predict roughly the correct amount of macroscopic hardening based upon the assumed hardening of individual crystals. (The E_T/H ratio is higher than that obtained from Taylor's classic aggregate theory[13], which neglects crystal elasticity. Taylor's result is $E_T = M^2H$, where M is the "Taylor factor", equal to 3.06 for f.c.c. crystals. The average of the tangent moduli near the ends of the half-cycles, where elastic strain increments have become insignificant relative to plastic strain increments, is approximately equal to Taylor's result.)

5.2 *Plastic work and latent energy*

Computer plots of accumulative values of (nondimensionalized) total work W, macroscopic (apparent) plastic work W_P, and internal plastic work Q within each cycle are shown in Figs. 3–6. Over the four cycles the ratio Q/W_P averages 91.4% with a mean deviation of 0.4%. Thus, *the model predicts that approximately 9% of the mechanically irrecoverable work W_p is stored as residual energy U_R.* In previous calculations of an aluminum model (Havner *et al.*[3]) we found U_R to be approximately 7% of W_p. The greater percentage of (average) residual strain

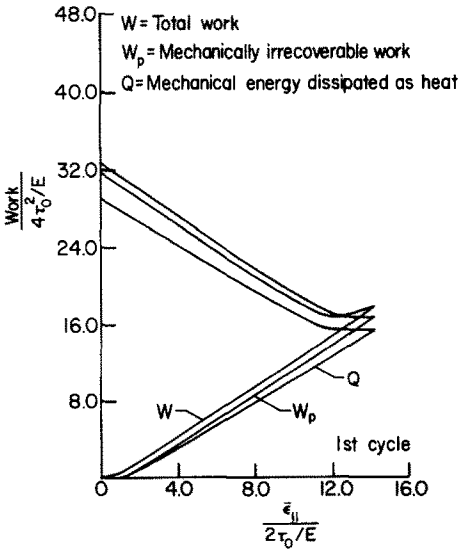

Fig. 3. Accumulative values of dimensionless work measures in first strain cycle of polycrystal model.

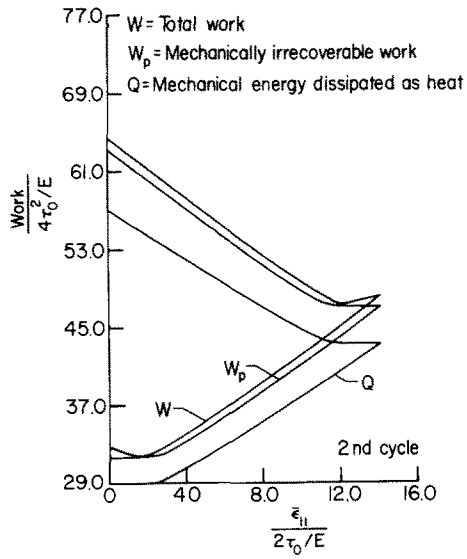

Fig. 4. Accumulative values of dimensionless work measures in second strain cyclic of polycrystal model.

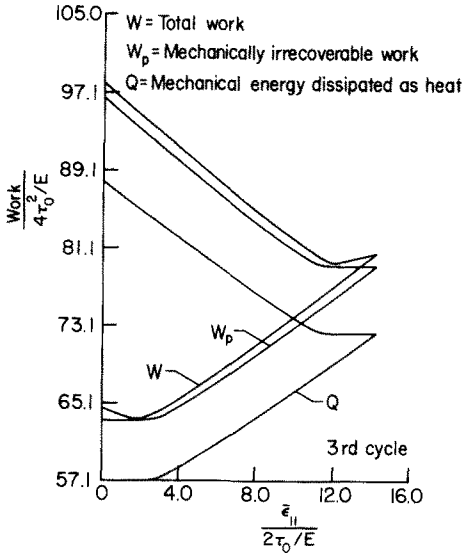

Fig. 5. Accumulative values of dimensionless work measures in third strain cycle of polycrystal model.

energy in the polycrystalline copper model is probably attributable to the greater elastic anisotropy of copper crystals.

The first noteworthy experimental study of heat generated during plastic deformation is the classic work of Farren and Taylor[25]. According to their measurements the latent energy averaged 7% in aluminum and 9% in copper, with mean deviations of 0.6 and 0.8% respectively. (Refer to their Table 3.) In subsequent investigations Taylor and Quinney[26] found this energy to range between 7.5 and 9% for a copper specimen in torsion up to very large strains, and Quinney and Taylor[27] determined the energy emitted on heating a twisted copper bar to be 9% (of prior plastic work). Measurements of latent energy in copper by Williams[28] and Wolfenden[24] agree with Farren and Taylor[25] at low to moderate strains. In aluminum, cyclic (small) strain and temperature measurements by Dillon[29] indicate a latent energy of 6%.

The close agreement between predictions of our polycrystalline model (both here and in Havner *et al.*[3]) and experimental results for latent energy is rather remarkable and possibly fortuitous. Aside from errors inherent in the numerical approximation, the residual strain energy U_R is only part of the latent energy determined experimentally, as previously noted (Section 4).

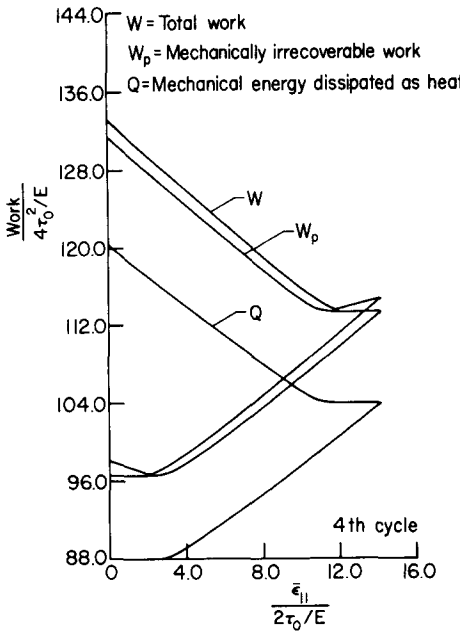

Fig. 6. Accumulative values of dimensionless work measures in fourth strain cycle of polycrystal model.

Moreover, most of the reported experimental results are for moderately large strains whereas our calculations are limited to very small deformations. It is of course conceivable that U_R (corresponding to gross lattice straining) dominates the latent energy at small strain, although U_R necessarily becomes insignificant as deformations grow large and the numbers of dislocations greatly multiply. (Refer to the original discussion of the latter point by Taylor[17].) Then, if total latent energy remains roughly a constant percentage of cold work into the moderate deformation range, the apparently fortuitous agreement between U_R as calculated here and experiment can be rationalized. However, we are not aware of any experimental information at small strain on the partitioning of latent energy between U_R and the submicroscale energy of dislocations. Thus, the above comments remain speculative.

6. CONCLUDING REMARKS

Although the close agreement between the results of our calculations on the discrete polycrystal model and published experimental values for each of (a) elastic properties, (b) aggregate hardening, and (c) residual strain energy may be in part fortuitous, we do not believe this can entirely be the case. Such consistent good fortune seems unlikely and some of the computational success in predicting macroscopic behavior should reasonably be credited to the heterogeneous model. Of course, a further subdivision of the individual crystallites into finite elements would have afforded some control over discretization errors. This might have enabled an assessment of the "goodness" of our simple characterization of individual crystal plasticity (viz. Taylor hardening and a constant slip system hardening modulus) divorced from the numerical approximation. However, we emphasize that it is the elastic and plastic *heterogeneity* of a representative volume element of polycrystalline material that accounts for its macroscopic plastic response. As we have seen here, even a very simple constitutive modeling of the individual crystals and a rather coarse overall aggregate approximation can represent much of the complexity of macroscopic material response.

Acknowledgement—Appreciation is expressed to the United States National Science Foundation, Solid Mechanics Program, for support of this work through Grant GK-31313.

REFERENCES

1. K. S. Havner, A discrete model for the prediction of subsequent yield surfaces in polycrystalline plasticity. *Int. J. Solids Structures* 7, 719 (1971).
2. K. S. Havner and R. Varadarajan, A quantitative study of a crystalline aggregate model. *Int. J. Solids Structures* 9, 379 (1973).

3. K. S. Havner, C. Singh and R. Varadarajan, Plastic deformation and latent strain energy in a polycrystalline aluminum model. *Int. J. Solids Structures* **10**, 861 (1974).
4. C. Singh, Theoretical studies of cyclic straining in polycrystalline metal plasticity. Ph.D. Thesis, North Carolina State University (1976).
5. G. R. Barsch, Adiabatic, isothermal and intermediate pressure derivatives of the elastic constants for cubic symmetry—I. Basic formulae. *Phys. Stat. Sol.* **19**, 129 (1967).
6. G. R. Barsch and Z. P. Chang, Adiabatic, isothermal and intermediate pressure derivatives of the elastic constants for cubic symmetry—II. Numerical results for 25 materials. *Phys. Stat. Sol.* **19**, 139 (1967).
7. R. Hill, The elastic behaviour of a crystalline aggregate. *Proc. Phys. Soc.* **A65**, 349 (1952).
8. R. F. S. Hearmon, *Applied Anisotropic Elasticity*, Chap. 3. Oxford University Press (1961).
9. J. W Hutchinson, Elastic-plastic behaviour of polycrystalline metals and composites. *Proc. R. Soc. Lond.* **A319**, 247 (1970).
10. Z. Hashin and S. Shtrikman, A variational approach to the theory of the elastic behaviour of polycrystals. *J. Mech. Phys. Solids* **10**, 343 (1962).
11. E. Kröner, B. K. Datta and D. Kessel, On the bounds of the shear modulus of macroscopically isotropic aggregates of cubic crystals, *J. Mech. Phys. Solids* **14**, 21 (1966).
12. G. I. Taylor, The distortion of crystals of aluminium under compression, Part II. *Proc. R. Soc. Lond.* **A116**, 16 (1927).
13. G. I. Taylor, Plastic strain in metals. *J. Inst. Metals* **62**, 307 (1938).
14. G. Maier, A minimum principle for incremental elastoplasticity with non-associated flow laws. *J. Mech. Phys. Solids* **18**, 319 (1970).
15. K. S. Havner, On unification, uniqueness, and numerical analysis in plasticity. Rept. 76-3, NSF Grants GK-31313 and ENG75-23662, North Carolina State University (1976).
16. R. Hill, The essential structure of constitutive laws for metal composites and polycrystals. *J. Mech. Phys. Solids* **15**, 79 (1967).
17. G. I. Taylor, Lattice distortion and latent heat of cold work in copper. Aeronautical Research Committee (1935). (Also: *The Scientific Papers of Sir Geoffrey Ingram Taylor* (edited by G. K. Batchelor), *Vol. I, Mechanics of Solids*, pp. 399–401. Cambridge University Press (1958).)
18. D. S. Kemsley and M. S. Paterson, The influence of strain amplitude on the work hardening of copper crystals in alternating tension and compression. *Acta Met.* **8**, 453 (1960).
19. R. O. Williams, The increase in internal energy of copper crystals during deformation at 25°C. *Acta Met.* **12**, 745 (1964).
20. H. P. Künzi and W. Krelle, *Nonlinear Programming*, Chap. 5. Blaisdell, Walton Mass. (1966).
21. O. De Donato and A. Franchi, A modified gradient method for finite element elastoplastic analysis by quadratic programming. *Comp. Meth. Appl. Mech. Engng.* **2**, 107 (1973).
22. B. Budiansky and T. T. Wu, Theoretical prediction of plastic strains of polycrystals. *Proc. 4th U.S. Natn. Cong. Appl. Mech.*, pp. 1175–1185, ASME (1962).
23. R. O. Williams, The stored energy of copper deformed at 24°C. *Acta Met.* **13**, 163 (1965).
24. A. Wolfenden, The energy stored in polycrystalline copper deformed at room temperature. *Acta Met.* **19**, 1373 (1971).
25. W. S. Farren and G. I. Taylor, The heat developed during plastic extension of metals. *Proc. R. Soc. Lond.* **A107**, 422 (1925).
26. G. I. Taylor and H. Quinney, The latent energy remaining in a metal after cold working. *Proc. R. Soc. Lond.* **A143**, 307 (1934).
27. H. Quinney and G. I. Taylor, The emission of the latent energy due to previous cold working when a metal is heated. *Proc. R. Soc. Lond.* **A163**, 157 (1937).
28. R. O. Williams, The stored energy in deformed copper. *Acta Met.* **9**, 949 (1961).
29. O. W. Dillon, Jr., Plastic deformation waves and heat generated near the yield point of annealed aluminum. *Mechanical Behavior of Materials under Dynamic Loads* (Edited by U. S. Lindholm), pp. 21-60. Springer, Berlin (1968).
30. G. Strang and G. J. Fix, *An Analysis of the Finite Element Method.* Prentice Hall, New Jersey (1973).
31. K. S. Havner and H. P. Patel, On convergence of the finite-element method for a class of elastic-plastic solids. *Quart. Appl. Math.* **34**, 59 (1976).

APPENDIX

Discrete Green's function and the self-straining problem

For generality, we present some details of the discrete "Green's function approach" for an arbitrary heterogeneous solid, corresponding to interpolating polynomials of any order. In the *self-straining* problem the body is fully constrained on a portion S_D of the surface and traction-free on the remainder S_F,† and the elastic response

$$\mathbf{u}_s = \mathbf{u}_s(\boldsymbol{\epsilon}^I), \quad \boldsymbol{\sigma}_s = \mathscr{L} \cdot (\boldsymbol{\epsilon}(\mathbf{u}_s) - \boldsymbol{\epsilon}^I) \tag{A1}$$

to an imposed inelastic strain (or strain increment) distribution $\boldsymbol{\epsilon}^I(x)$ is to be determined.

Let $G_{pm}(x', x)$ denote the displacement u_p at x' due to a unit force F_m at x, and consider interpolating polynomials $\phi_M(x)$ *with a local basis* corresponding to a finite-element subdivision of the heterogeneous body (making certain that no element cuts across a material interface). Then

$$\mathbf{G}(x', x) = \sum \phi_M(x') \mathbf{G}(x_M, x) \tag{A2}$$

where $\mathbf{G}(x_M, x)$ is the *discrete Green's function* at nodal point M. (Henceforth upper case subscripts denote nodal points and lower case subscripts denote Cartesian components.) The continuous, piecewise polynomials $\phi_M(x)$ must of course satisfy $\phi_M(x_J) = \delta_{MJ}$ (the Kronecker delta), $\Sigma \phi_M(x) = 1$ (summation on all nodes), and $\phi_M(x) = 0$ for points M and x having no element in common.

†The mixed boundary conditions of the polycrystal model are of course accommodated by assigning individual component pairs of force and displacement (at a boundary point) to S_D and S_F as appropriate.

Let $\nabla' \mathbf{G}(x', x)$, with components $\partial'_q G_{pm}(x', x)$, denote the gradient of $\mathbf{G}(x', x)$ with respect to position x'. Then, the formal solution of the self-straining displacement field is (from virtual work)

$$\mathbf{u}^s(x) = \int \{\mathscr{L}(x') \cdot \nabla' \mathbf{G}(x', x)\} \cdot \boldsymbol{\epsilon}^I(x')\, dV'$$

or

$$u_m^s(x) = \int \mathscr{L}_{klpq}(x') \partial'_q G_{pm}(x', x) \epsilon^I_{kl}(x')\, dV'. \tag{A3}$$

Thus, from (A1),

$$\sigma^s_{ij}(x) = -\int Z_{ijkl}(x, x') \epsilon^I_{kl}(x')\, dV' \tag{A4}$$

where the kernel inflence function $\mathbf{Z}(x, x')$ may be expressed

$$Z_{ijkl}(x, x') = \mathscr{L}_{ijkl}(x) \delta(x, x') - \mathscr{L}_{ijmn}(x) \partial_n \partial'_q G_{mp}(x, x') \mathscr{L}_{pqkl}(x'). \tag{A5}$$

Here we have utilized the symmetries of the elastic moduli and the basic reciprocity relations of the Green's function (viz. $G_{pm}(x', x) = G_{mp}(x, x')$) and have introduced the Dirac-delta function $\delta(x, x')$, scaled such that $\int \delta(x, x') f(x')\, dV' = f(x)$. Observe that $\mathbf{Z}(x, x')$ also has the reciprocal property

$$Z_{ijkl}(x, x') = Z_{klij}(x', x). \tag{A6}$$

The approximate Green's function $\mathbf{G}_m(x', x)$ (due to $F_m(x) = 1$) may be determined from the minimization of

$$2I_1(\mathbf{w}) = a(\mathbf{w}, \mathbf{w}) - 2w_m(x), \quad m = 1, 2, 3, \tag{A7}$$

over the admissible class of continuous, piecewise polynomials $\mathbf{w}(x') = \Sigma\, \phi_J(x') \mathbf{w}_J$, where $a(\mathbf{w}, \mathbf{w})$ is the positive-definite quadratic form

$$a(\mathbf{w}, \mathbf{w}) = \int \partial \mathbf{w} \cdot \mathscr{L} \cdot \partial \mathbf{w}\, dV. \tag{A8}$$

Equivalently, from the discrete virtual work equation on the admissible class,

$$a(\mathbf{w}, \mathbf{G}_m) = w_m(x), \tag{A9}$$

(corresponding to $F_m(x) = 1$) we find, following the usual procedure,

$$\mathbf{G}(x_M, x) = \sum \mathbf{K}^{-1}_{MJ} \phi_J(x), \tag{A10}$$

where

$$(K_{JM})_{mp} = \int \frac{\partial \phi_J}{\partial x_n} \mathscr{L}_{mnpq} \frac{\partial \phi_M}{\partial x_q}\, dV \tag{A11}$$

is an element of the *overall stiffness matrix* $\mathbf{K}$ (symmetric, positive-definite). Thus, upon substituting (A2) and (A10) into (A5), the final (approximate) solution for the kernel $\mathbf{Z}(x, x')$ is

$$Z_{ijkl}(x, x') = \mathscr{L}_{ijkl}(x) \delta(x, x') - \mathscr{L}_{ijmn}(x) \sum \sum \frac{\partial \phi_J(x)}{\partial x_n} \frac{\partial \phi_M(x')}{\partial x'_q} (K^{-1}_{JM})_{mp} \mathscr{L}_{pqkl}(x'). \tag{A12}$$

Suppose all finite elements to be of equal order-of-magnitude in size and let h denote a representative element dimension. The Green's function of the finite element solution (which we now denote $\mathbf{G}^h(x, x')$ to distinguish it from the exact Green's function) may be expressed (combining (A2) and (A10))

$$\mathbf{G}^h(x, x') = \sum \sum \phi_J(x) \phi_M(x') \mathbf{K}^{-1}_{JM}. \tag{A13}$$

Denoting the degree of the (complete) polynomials $\phi_J(x)$ by n, it may be shown (following arguments similar to those in Strang and Fix [30, pp. 39–40 and 106]) that

$$0 \le a(\mathbf{G}_m - \mathbf{G}_m{}^h, \mathbf{G}_m - \mathbf{G}_m{}^h) \le 0(h^{2n}). \tag{A14}$$

Thus, the approximate Green's function of (A13) converges. (For piecewise linear polynomials, the right-hand side of (A14) is of course $0(h^2)$.) A proof of convergence for the *overall elastic-plastic incremental boundary value problem* which applies to the present polycrystal model has been given by Havner and Patel[31].